

ARTICLES

Skp2 targeting suppresses tumorigenesis by Arf-p53-independent cellular senescence

Hui-Kuan Lin^{1,2,3}, Zhenbang Chen^{1,2,4,†}, Guocan Wang^{1,2,4*}, Caterina Nardella^{1,2,4*}, Szu-Wei Lee^{3*}, Chan-Hsin Chan³, Wei-Lei Yang³, Jing Wang³, Ainara Egia⁴, Keiichi I. Nakayama⁵, Carlos Cordon-Cardo^{2,†}, Julie Teruya-Feldstein² & Pier Paolo Pandolfi^{1,2,4}

Cellular senescence has been recently shown to have an important role in opposing tumour initiation and promotion. Senescence induced by oncogenes or by loss of tumour suppressor genes is thought to critically depend on induction of the p19^{Arf}-p53 pathway. The Skp2 E3-ubiquitin ligase can act as a proto-oncogene and its aberrant overexpression is frequently observed in human cancers. Here we show that although Skp2 inactivation on its own does not induce cellular senescence, aberrant proto-oncogenic signals as well as inactivation of tumour suppressor genes do trigger a potent, tumour-suppressive senescence response in mice and cells devoid of Skp2. Notably, Skp2 inactivation and oncogenic-stress-driven senescence neither elicit activation of the p19^{Arf}-p53 pathway nor DNA damage, but instead depend on Atf4, p27 and p21. We further demonstrate that genetic Skp2 inactivation evokes cellular senescence even in oncogenic conditions in which the p19^{Arf}-p53 response is impaired, whereas a Skp2-SCF complex inhibitor can trigger cellular senescence in p53/Pten-deficient cells and tumour regression in preclinical studies. Our findings therefore provide proof-of-principle evidence that pharmacological inhibition of Skp2 may represent a general approach for cancer prevention and therapy.

Cellular senescence represents an irreversible form of cell-cycle arrest that can be triggered by a variety of insults. Induction of cellular senescence (for example, by oncogenic Ras) results in p19^{Arf} (encoded by the *Ink4a/Arf* locus, also known as *Cdkn2a* locus) and p53 accumulation, which is critical for this senescence response. Recent studies suggest that cellular senescence can act as an important tumour-suppressive mechanism to restrict tumour development *in vivo*^{1–7}.

Inactivation of Pten functions is frequently observed in human cancers^{8–10}. Although Pten negatively regulates cell proliferation and survival, we surprisingly discovered that acute *Pten* inactivation triggers the accumulation of p19^{Arf}-p53 and cellular senescence². Concomitant inactivation of *p53* (also known as *Trp53* in mice, and *TP53* in humans) and *Pten* abrogates this senescence response, in turn promoting invasive and lethal prostate cancer². Although these findings further underscore the critical importance of the cellular senescence *Arf*-*p53* failsafe pathway, the frequent loss or mutation of *ARF* or *P53* in human cancers would compromise the tumour-suppressive efficacy of this response, thereby limiting therapeutic potential.

Skp2 is a critical component of the Skp2-SCF complex, which acts as an E3 ligase to target p27 and other substrates for ubiquitylation and degradation^{11,12}. Recent studies suggest that Skp2 may have oncogenic activity^{13–16}. Notably, SKP2 overexpression is frequently observed in human cancer^{11,12,17}, strongly suggesting that SKP2 overexpression may contribute to tumorigenesis. *Skp2*-knockout mice are viable and fertile¹⁸. Hence, specific inactivation of *Skp2* may represent an appealing therapeutic modality. Here we show that *Skp2* inactivation profoundly restricts tumorigenesis by eliciting cellular

senescence only in oncogenic conditions. Remarkably, this senescence response is triggered in a p19^{Arf}-p53-independent manner. Skp2 pharmacological inactivation may therefore represent a general approach towards a ‘pro-senescence’ therapy for cancer prevention and treatment.

Skp2 loss restores cellular senescence by Ras and E1A

Skp2 deficiency delays cell cycle progression^{11,12}. We therefore asked whether *Skp2* deficiency would trigger cellular senescence. We isolated mouse embryonic fibroblasts (MEFs) from wild-type and *Skp2*^{-/-} mice and determined cellular senescence in these cells by senescence-associated β -galactosidase (SA- β -gal) staining. Although *Skp2*^{-/-} MEFs proliferated less than wild-type MEFs (Supplementary Fig. 1e)^{11,12}, cellular senescence in *Skp2*^{-/-} MEFs was comparable to that in the wild-type MEFs (Supplementary Fig. 1a). In contrast, acute inactivation of *Pten* in MEFs markedly increased cellular senescence as previously reported (Supplementary Fig. 1a)². Thus, *Skp2* deficiency by itself does not elicit cellular senescence.

Ectopic overexpression of proto-oncogenic Ras (Ras(G12V)) in MEFs elicits cellular senescence through the p19^{Arf}-p53 pathway^{19,20}. Simultaneous co-expression of E1A and Ras in MEFs overcomes Ras-induced senescence by preventing activation of the p19^{Arf}-p53 pathway and resulting in oncogenic transformation²⁰. Thus, E1A enables Ras to overcome the cellular senescence response. As Skp2 also cooperates with oncogenic Ras to induce cell transformation¹³, it is conceivable that Skp2 might also display its oncogenic activity by antagonizing Ras-induced cellular senescence. On this basis, we tested whether endogenous Skp2 activity is required for cellular transformation induced by Ras and E1A. Although cellular senescence was not

¹Cancer Biology and Genetics Program, ²Department of Pathology, Sloan-Kettering Institute, Memorial Sloan-Kettering Cancer Center, 1275 York Avenue, New York, New York 10021, USA. ³Department of Molecular and Cellular Oncology, The University of Texas M.D. Anderson Cancer Center, Houston, Texas 77030, USA. ⁴Cancer Genetics Program, Beth Israel Deaconess Cancer Center and Department of Medicine, Beth Israel Deaconess Medical Center, Harvard Medical School, 330 Brookline Avenue, Boston, Massachusetts 02215, USA. ⁵Department of Molecular and Cellular Biology, Medical Institute of Bioregulation, Kyushu University, Fukuoka, Fukuoka 812-8582, Japan. †Present addresses: Department of Biochemistry and Cancer Biology, Meharry Medical College, 1005 Dr D. B. Todd Jr Boulevard, Nashville, Tennessee 37208-3599, USA (Z.C.); Irving Cancer Research Center, Room 309, 1130 St. Nicholas Avenue, New York, New York 10032, USA (C.C.-C.).

*These authors contribute equally to this work.

observed in wild-type MEFs after Ras and E1A overexpression, *Skp2* deficiency triggered cellular senescence (Supplementary Fig. 1b, c). We also found that the ability of Ras to induce cellular senescence was far greater in *Skp2*^{-/-} MEFs than in wild-type MEFs (Supplementary Fig. 1b, c). It should be noted that the induction of p19^{Arf} and p53 protein levels in *Skp2*^{-/-} MEFs by Ras was comparable if not lower than that of wild-type MEFs (Supplementary Fig. 1d). Moreover, *Skp2* inactivation profoundly restricted cell proliferation and transformation after Ras and E1A overexpression (Supplementary Fig. 1e, f). Thus, *Skp2* inactivation triggers cellular senescence in the presence of powerful oncogenic signals, even when the p19^{Arf}-p53 response is evaded.

Skp2 loss causes senescence in *Pten*^{+/-} and *Arf*^{-/-} mutants

We assessed whether *Skp2* inactivation would trigger cellular senescence even when cells experience loss of major tumour-suppressive networks such as those controlled by *Pten* and p19^{Arf}-p53. To this end, we crossed *Skp2*^{-/-} mutants with *Pten*^{+/-} and *Arf*^{-/-} mutants. The resulting compound mice were further intercrossed to generate MEFs of different genotypes for cell proliferation and senescence assays. As aforementioned, *Skp2*^{-/-} MEFs grew much slower than wild-type MEFs, whereas wild-type and *Pten*^{+/-} MEFs grew comparably (Supplementary Fig. 2a). No obvious cellular senescence was observed in wild-type, *Pten*^{+/-} and *Skp2*^{-/-} MEFs (Fig. 1a). Surprisingly, *Pten*^{+/-} *Skp2*^{-/-} MEFs had a slower growth rate than *Skp2*^{-/-} MEFs and exhibited full-blown characteristics of cellular senescence such as flattened large cells and positive SA- β -gal staining (Fig. 1a and Supplementary Fig. 2a). We also detected cellular senescence in *Pten*^{+/-} *Skp2*^{-/-} MEFs under hypoxic conditions (Supplementary Fig. 2b). We did not see cooperation between *Pten* inactivation and *Skp2* deficiency in triggering apoptosis, although *Skp2*^{-/-} MEFs had a higher rate of apoptosis than wild-type MEFs (Supplementary Fig. 3a)¹⁸. However, the apoptosis rate in the prostate of *Pten*^{+/-} *Skp2*^{-/-} mice was higher than in wild-type, *Pten*^{+/-} and *Skp2*^{-/-} mice (see later and Supplementary Fig. 3b).

As cellular senescence is largely dependent on activation of the p19^{Arf}-p53 pathway in MEFs^{21,22}, we determined whether this pathway is activated in *Pten*^{+/-} *Skp2*^{-/-} MEFs. Notably, we found that p19^{Arf} and p53 protein levels in *Pten*^{+/-} *Skp2*^{-/-} MEFs were comparable to levels in wild-type MEFs (Fig. 1b and Supplementary Fig. 4), suggesting that the p19^{Arf}-p53 pathway may not be involved in the senescence response in *Pten*^{+/-} *Skp2*^{-/-} MEFs. To test this hypothesis further, we exposed MEFs of various genotypes to two well-established p53-inactivating tools: a short hairpin RNA (shRNA) against p53 (ref. 23) or a dominant-negative p53 mutant (p53-DN)²⁴. Notably, in both conditions cell growth was promoted in wild-type and *Pten*^{-/-} MEFs (Supplementary Fig. 5a, b), but neither of them overcame the cellular senescence nor the growth arrest in *Pten*^{+/-} *Skp2*^{-/-} MEFs (Fig. 1c and Supplementary Fig. 5c), suggesting that *Skp2* deficiency cooperates with *Pten* inactivation to trigger a new senescence response by a p19^{Arf}-p53-independent pathway.

p19^{Arf} induction is required for cellular senescence in MEFs in the context of acute *Pten* inactivation²⁵, whereas loss of p19^{Arf} leads to cell immortalization^{21,22}. We investigated whether *Skp2* inactivation could elicit cellular senescence in an *Arf*-deficient genetic background. Notably, *Arf*^{-/-} *Skp2*^{-/-} MEFs showed massive cellular senescence similar to *Pten*^{+/-} *Skp2*^{-/-} MEFs (Fig. 1d). Moreover, p53 expression was not induced in *Arf*^{-/-} *Skp2*^{-/-} MEFs (Supplementary Fig. 6a). This cellular senescence profoundly suppressed the growth of *Arf*^{-/-} MEFs (Supplementary Fig. 6b). *Skp2* deficiency also induced cellular senescence after p53 inactivation (Supplementary Fig. 6c, d).

DNA damage has been recently associated with cellular senescence²⁶⁻²⁸. However, we found no evidence of DNA-damage-response activation in *Pten*^{+/-} *Skp2*^{-/-} MEFs, as determined by the levels of phosphorylated-(S15)-p53 and - γ -H2ax (also known as γ -H2afx) (Supplementary Fig. 4). Collectively, these results support the notion that *Skp2* inactivation can trigger a new type of

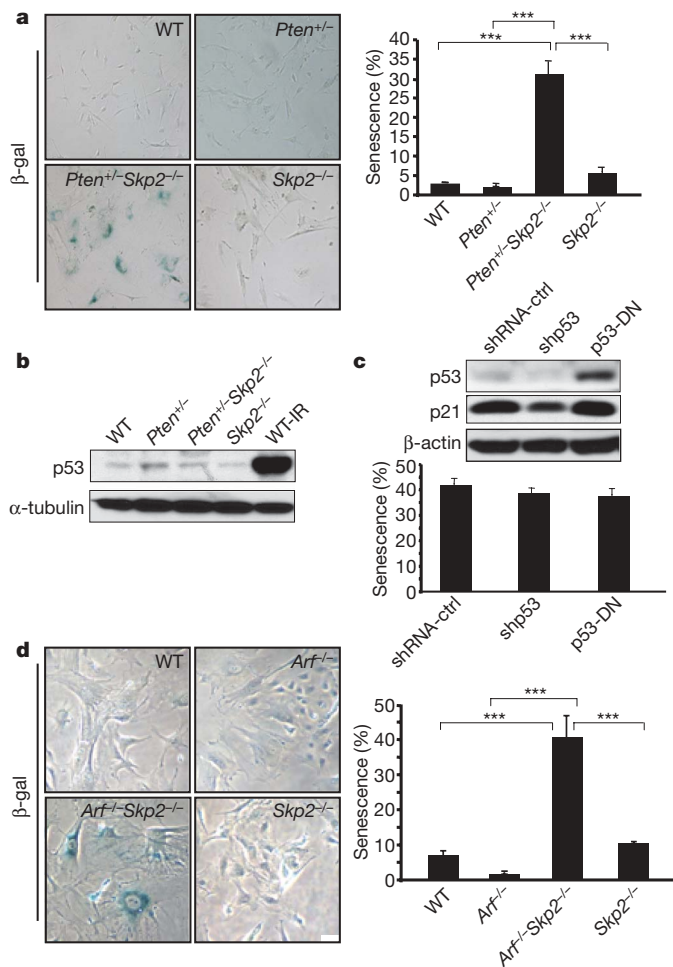


Figure 1 | *Skp2* loss triggers a new senescence response in MEFs in the context of *Pten* inactivation and *Arf* deficiency by a p19^{Arf}-p53-independent pathway. **a**, Primary MEFs at passage 5 from various mouse embryos were plated for senescence assay. WT, wild type. **b**, Cell lysates were collected from primary MEFs of various genotypes of mouse embryos for western blot analysis. The lysates from wild-type MEFs treated with γ -irradiation for 60 min served as a positive control for p53. **c**, Primary *Pten*^{+/-} *Skp2*^{-/-} MEFs infected with retroviruses expressing various control shRNA (shRNA-ctrl), p53 shRNA (shp53), or dominant-negative p53 (p53-DN) were plated for senescence assay and western blot analysis. **d**, Primary MEFs at passage 5 from various genotypes of mouse embryos were plated for senescence assay. Results are presented as mean \pm s.d. from a representative experiment performed in triplicate. ****P* < 0.001 using two-tailed Student's *t*-test, *n* = 3.

cellular senescence that does not involve DNA damage and can suppress transformation even when the p19^{Arf}-p53 response is impaired.

p27, p21 and Atf4 induction contribute to senescence

We next examined the molecular mechanism by which *Skp2* deficiency synergizes with oncogenic insults to trigger cellular senescence. Although p53 and p19^{Arf} levels remained unchanged, we found that *Skp2* deficiency cooperated with *Pten* inactivation or *Arf* loss to induce p27 expression (Fig. 2a, b). p21 expression was also increased in *Pten*^{+/-} *Skp2*^{-/-} and *Arf*^{-/-} *Skp2*^{-/-} MEFs (Fig. 2a, b). E2F1, cyclin D1 and Cdt1, involved in cell cycle progression and DNA replication, are also targets for *Skp2* (refs 12, 29). We found that cyclin D1, but not E2F1 and Cdt1, were induced in *Pten*^{+/-} *Skp2*^{-/-} MEFs (Supplementary Fig. 7a). Because cyclin D1 promotes cell cycle progression, its upregulation is unlikely to be involved in mediating senescence in *Pten*^{+/-} *Skp2*^{-/-} MEFs.

Endoplasmic reticulum (ER) stress proteins such as BiP (also known as Hspa5 or GRP78), phospho-Perk (p-Perk), and Atf4 are induced after oncogenic insults and have an important role in cellular

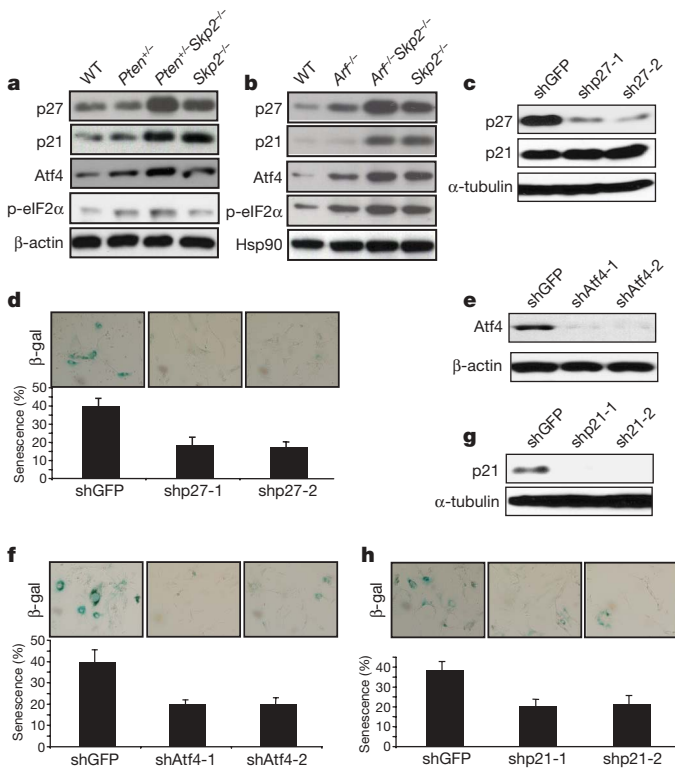


Figure 2 | Upregulation of p27, p21 and Atf4 drives cellular senescence in *Pten*^{+/-} *Skp2*^{-/-} and *Arf*^{-/-} *Skp2*^{-/-} MEFs. **a, b**, Cell lysates were collected from primary MEFs of various genotypes of mouse embryos for western blot analysis. **c, d**, *Pten*^{+/-} *Skp2*^{-/-} MEFs at passage 2 infected with lentiviruses expressing green fluorescent protein (GFP) shRNA (shGFP) or p27 shRNA (shp27-1 and -2) were plated for western blot analysis (**c**) and senescence assay (**d**). Results are mean \pm s.d. from a representative experiment performed in triplicate. **e, f**, *Pten*^{+/-} *Skp2*^{-/-} MEFs at passage 2 infected with lentiviruses expressing GFP shRNA or *Atf4* shRNA were plated for western blot analysis (**e**) and senescence assay (**f**). **g, h**, *Pten*^{+/-} *Skp2*^{-/-} MEFs at passage 2 infected with lentiviruses expressing GFP shRNA or p21 shRNA were plated for western blot analysis (**g**) and senescence assay (**h**).

senescence³⁰. We did not find a significant increase in BiP or p-Perk (Supplementary Fig. 7b and data not shown) in *Pten*^{+/-} *Skp2*^{-/-} MEFs. In contrast, *Atf4* was markedly induced in *Pten*^{+/-} *Skp2*^{-/-} MEFs (Fig. 2a). Likewise, we also observed a marked increase in *Atf4* protein levels, but not p-Perk, in *Arf*^{-/-} *Skp2*^{-/-} MEFs (Fig. 2b and Supplementary Fig. 7c). The induction of *Atf4* protein levels in *Pten*^{+/-} *Skp2*^{-/-} MEFs was not accompanied by messenger RNA upregulation, nor by the enhanced *Atf4* protein stability (Supplementary Fig. 8 and data not shown). Instead, we observed an increase in phosphorylated eIF2 α (p-eIF2 α ; also known as p-Eif2s1) in *Pten*^{+/-} *Skp2*^{-/-} and *Arf*^{-/-} *Skp2*^{-/-} MEFs compared to wild-type cells (Fig. 2a, b). Because p-eIF2 α positively regulates *Atf4* translation³¹, our results indicate that *Atf4* upregulation is probably triggered by the enhancement of p-eIF2 α levels.

As p27, p21 and *Atf4* were induced in both *Pten*^{+/-} *Skp2*^{-/-} and *Arf*^{-/-} *Skp2*^{-/-} MEFs, we next determined whether their upregulation contributes to senescence. p27 (also known as *Cdkn1b*) shRNA efficiently abrogated p27 expression and partially rescued growth arrest and cellular senescence in *Pten*^{+/-} *Skp2*^{-/-} MEFs (Fig. 2c, d and Supplementary Figs 9a, b and 10a). Similarly, knockdown of *Atf4* or p21 (also known as *Cdkn1a*) in these cells also partially reversed cellular senescence and cell arrest (Fig. 2e–h and Supplementary Figs 9c and 10b, c). Concomitant knockdown of *Atf4*, p21 and p27 in these cells reversed cellular senescence more efficiently than their individual knockdown (Supplementary Fig. 10d). In contrast, in *Skp2*^{-/-} MEFs, p27 knockdown accelerated growth whereas *Atf4* knockdown did not (Supplementary Fig. 10e, f). These results

strongly indicate that the concomitant upregulation of p27, p21 and *Atf4* is a required and powerful engine for the induction of cellular senescence upon *Skp2* inactivation.

Skp2 loss restricts tumorigenesis independently of *Arf*-p53

We found that inactivation of *Skp2* in the presence of an oncogenic stress results in the induction of cellular senescence that opposes transformation *in vitro* even when the p19^{Arf}-p53 response is impaired. We next determined whether *Skp2* loss restricts tumorigenesis *in vivo* through similar mechanisms, and first analysed tumorigenesis in *Skp2*^{-/-} *Pten*^{+/-} compound mutants (Supplementary Fig. 11a). Although *Pten* heterozygous inactivation reduced lifespan in mice, compound *Skp2* deficiency prolonged overall survival (Fig. 3a). *Pten*^{+/-} mice develop lymphadenopathy and adrenal tumours (pheochromocytoma) at complete penetrance^{32,33}. As expected, *Pten*^{+/-} mice developed adrenal tumours with 100% penetrance by 1 year of age, whereas *Skp2* loss remarkably abrogated adrenal tumour formation in compound mutants ($P < 0.0001$; Fig. 3b, top, c and Supplementary Fig. 11b). *Pten* protein expression in adrenal tissues was comparable between wild-type, *Pten*^{+/-} and *Pten*^{+/-} *Skp2*^{-/-} mice, before or after tumour occurrence, suggesting that there is no loss of heterozygosity at the *Pten* locus in the adrenal tissues in any of these mutants and conditions (Supplementary Fig. 11c). Lymphadenopathy after *Pten* inactivation was also profoundly inhibited by *Skp2* loss ($P < 0.01$; Fig. 3b,

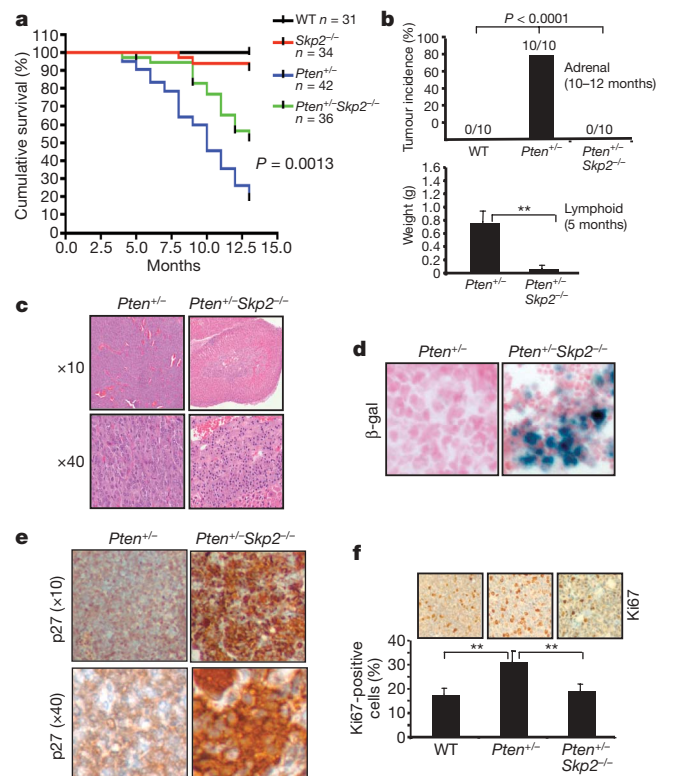


Figure 3 | *Skp2* deficiency restricts tumorigenesis after *Pten* inactivation by inducing cellular senescence *in vivo*. **a**, Kaplan–Meier plot analysis of cumulative survival of indicated mouse genotypes. **b**, Top, adrenal tissues from various mouse genotypes (10–12 months) were analysed for tumorigenesis; bottom, lymphoid tissues within the neck were obtained and weighed from female mice of various genotypes (around 5 months). $**P < 0.01$ using two-tailed Student's *t*-test, $n = 6$. **c**, Histological analysis of adrenal tissues from 12-month-old *Pten*^{+/-} and *Pten*^{+/-} *Skp2*^{-/-} mice. *Pten*^{+/-} mice developed adrenal tumour (pheochromocytoma), which was profoundly inhibited in *Pten*^{+/-} *Skp2*^{-/-} mice. **d**, Senescence analysis of lymphoid tissue from 5-month-old *Pten*^{+/-} and *Pten*^{+/-} *Skp2*^{-/-} mice. **e**, Lymphoid tissues from 5-month-old mice of the indicated genotypes were obtained for p27 immunohistochemistry. **f**, Quantification of Ki67 staining of lymphoid tissues from 5-month-old mice. Results are mean \pm s.d. $**P < 0.01$ using two-tailed Student's *t*-test, $n = 3$.

bottom and Supplementary Fig. 11d). Tumorigenesis was also markedly suppressed in other organs (for example, in the prostate, where the prostatic intraepithelial neoplasia (PIN) incidence was profoundly restricted by *Skp2* inactivation; data not shown).

To determine whether *Skp2* inactivation along with *Pten* inactivation would trigger cellular senescence *in vivo*, we performed SA- β -gal staining in the few hyperplastic lymphoid lesions still identified in *Pten*^{+/-} *Skp2*^{-/-} mice (see, for example, Supplementary Fig. 10d). We observed both cellular senescence and p27 induction in the lymphoid tissues from *Pten*^{+/-} *Skp2*^{-/-} mice (Fig. 3d, e and Supplementary Fig. 12), which inversely correlated with cell proliferation (Fig. 3f).

We then examined whether *Skp2* inactivation would also restrict tumorigenesis after *Arf* loss by crossing *Skp2*^{-/-} with *Arf*^{-/-} mice (Supplementary Fig. 13). *Skp2* inactivation markedly prolonged the overall survival of *Arf*^{-/-} mice (Fig. 4a). Around 33% of *Arf*^{-/-} mice developed sarcoma and/or lymphoma within 1 year (Fig. 4b–d)^{34,35}. In contrast, none of the *Arf*^{-/-} *Skp2*^{-/-} compound mutant mice showed signs of tumour formation ($P < 0.02$; Fig. 4b–d).

Senescence after *Pten* and *Skp2* inactivation in the prostate

Complete *Pten* inactivation in the prostate triggers a tumour-suppressive cellular senescence response². We therefore examined whether this response could be further potentiated by *Skp2* loss and affect tumorigenesis after complete *Pten* inactivation in the prostate. For prostate-specific inactivation, we made use of Cre-*loxP*-mediated recombination and probasin (*Pbsn*, also known as *PB*)-*Cre4* transgenic mice expressing the Cre recombinase after puberty in the prostatic epithelium². We obtained *Pten*^{loxP/loxP}; *PB*-*Cre4* and *Pten*^{loxP/loxP} *Skp2*^{-/-}; *PB*-*Cre4* compound mutant mice, hereafter referred to as *Pten*^{pc-/-} and *Pten*^{pc-/-} *Skp2*^{-/-} mice, respectively (Supplementary Fig. 14a). Although complete *Pten* inactivation in

mouse prostates leads to invasive prostate cancers, it does not affect overall survival². We did not detect a difference in overall survival between *Pten*^{pc-/-} and *Pten*^{pc-/-} *Skp2*^{-/-} mice (Supplementary Fig. 14b).

Prostate cancer development in these mice was monitored by magnetic resonance imaging (MRI) and histopathological analysis. Consistent with our previous findings², MRI analysis showed prostate tumour masses in *Pten*^{pc-/-} mice at 6 months of age, which were significantly reduced in *Pten*^{pc-/-} *Skp2*^{-/-} mice (Supplementary Fig. 14c). The average size of the prostate in *Pten*^{pc-/-} mice was tenfold larger than in wild-type mice, whereas complete *Skp2* loss markedly reduced tumour weight after complete *Pten* inactivation (Fig. 5a). Histological analysis showed that *Skp2* loss inhibited invasive prostate cancer after *Pten* inactivation, albeit PIN lesions were still observed in *Pten*^{pc-/-} *Skp2*^{-/-} mice (Supplementary Fig. 14d, e). Furthermore, this suppressive effect by *Skp2* loss was persistent, as we also observed a profound reduction in tumour weight and invasive prostate cancer in *Pten*^{pc-/-} *Skp2*^{-/-} mice at 15 months of age (Supplementary Fig. 14f, g).

We next investigated, *in vivo*, the molecular basis for tumour suppression elicited by *Skp2* inactivation. We found that p27 protein expression was synergistically induced in prostates from compound mutants, as determined by immunohistochemistry and western blot analysis (Supplementary Fig. 15a, b), whereas p53 expression was comparably induced in *Pten*^{pc-/-} and *Pten*^{pc-/-} *Skp2*^{-/-} mice

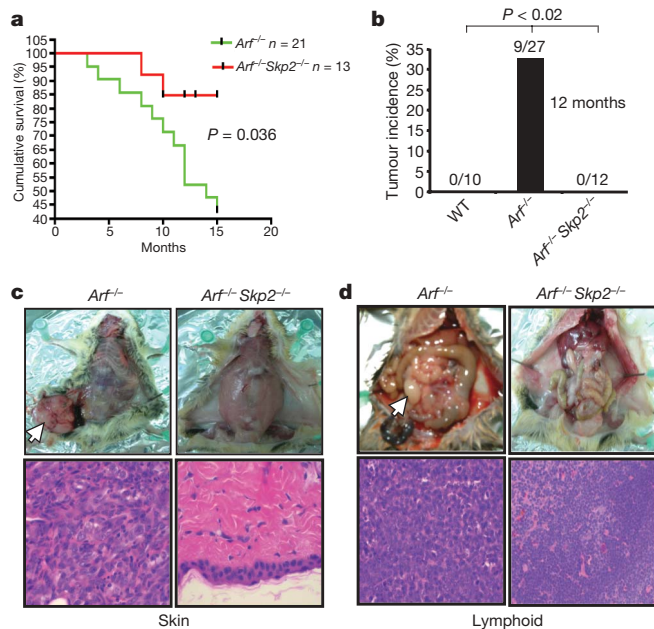


Figure 4 | *Skp2* inactivation restricts tumorigenesis upon *Arf* deficiency. **a**, Kaplan–Meier plot analysis of cumulative survival of *Arf*^{-/-} and *Arf*^{-/-} *Skp2*^{-/-} mice. **b**, A cohort of wild-type, *Arf*^{-/-} and *Arf*^{-/-} *Skp2*^{-/-} mice were analysed for tumorigenesis within a 1-year period. *Arf*^{-/-} *Skp2*^{-/-} mice did not develop any tumour up to 1 year observation. Nine out of twenty-seven *Arf*^{-/-} mice developed either sarcoma or lymphomas, whereas none of 12 *Arf*^{-/-} *Skp2*^{-/-} mice developed tumours. The statistic was analysed by chi-squared test, χ^2 . **c**, Histopathological analysis of skin tissues from *Arf*^{-/-} and *Arf*^{-/-} *Skp2*^{-/-} mice at 1 year old. Arrow indicates sarcoma. **d**, Histopathological analysis of lymphoid tissues lymphoid tissues from *Arf*^{-/-} and *Arf*^{-/-} *Skp2*^{-/-} mice at 1 year of age. The arrow indicates lymphoma. Original magnification, $\times 40$ (**c**, **d**).

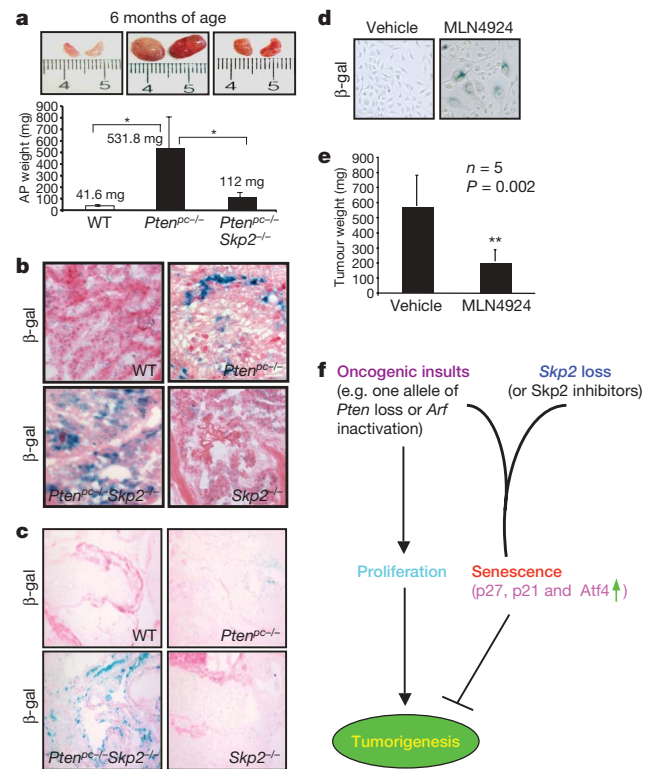


Figure 5 | *Skp2* deficiency restricts prostate cancer development by triggering cellular senescence *in vivo*. **a**, Biopsy of anterior prostate (AP) tumours at 24 weeks from various genotypes of mice and their actual sizes and weights. Results are mean \pm s.d. * $P < 0.05$ using two-tailed Student's *t*-test, $n = 5$. **b**, **c**, Senescence analysis of anterior prostate from *Pten*^{pc-/-} and *Pten*^{pc-/-} *Skp2*^{-/-} mice aged 3 months (**b**) or 15 months (**c**). A representative section from three mice is presented for each genotype. Original magnifications, $\times 40$ (**b**) and $\times 20$ (**c**). **d**, PC3 cells were treated with vehicle or 0.1 μ M MLN4924 for 4 days and collected for cellular senescence assay. **e**, Nude mice bearing PC3 xenograft tumours (around 300 mm³) were treated with vehicle or MLN492, and tumour weight was measured. **f**, Working model for tumour-suppressive cellular senescence driven by oncogenic insults and *Skp2* deficiency.

(Supplementary Fig. 15c). *Skp2* deficiency profoundly enhanced cellular senescence upon *Pten* inactivation (Fig. 5b). This was observed at earlier time points and inversely correlated with cell proliferation (Supplementary Fig. 16a, b). Notably, this response was also sustained over time. We could detect massive β -gal positivity in prostates from *Pten^{pc-/-} Skp2^{-/-}* mice even at 15 months of age, whereas β -gal positivity was barely detected at that age in prostates from *Pten^{pc-/-}* mice (Fig. 5c). Thus, *Skp2* inactivation potentiates and sustains over time the senescence response elicited by an oncogenic stimulus, suggesting that pharmacological inhibition of *Skp2* may be used as a powerful pro-senescence approach for cancer therapy and chemoprevention.

Skp2-SCF complex inactivation triggers senescence

To corroborate the potential use of such an approach for cancer therapy, we determined whether pharmacological inactivation of the Skp2-SCF complex induces cellular senescence in p53-deficient cells and, importantly, suppresses the growth of the pre-formed tumours. To this end, we took advantage of MLN4924 (ref. 36)—an inhibitor for the neddylation of cullin 1, which is a component of Skp2-SCF complex. We used PC3 prostate cancer cells for this pre-clinical analysis because these cells are both p53-null and *Pten*-null, hence representing one of the most aggressive genetic states encountered in human cancer. Remarkably, treatment of MLN4924 in PC3 cells triggered cellular senescence (Fig. 5d). Moreover, the growth of PC3 tumours treated with MLN4924 *in vivo* was also suppressed (Fig. 5e). Coherent with these findings, *Skp2* silencing in PC3 and in DU145 prostate cancer cells, which have also evaded the p53 response, triggered cellular senescence and cooperated with the DNA-damaging agent doxorubicin to induce cellular senescence and growth arrest (Supplementary Fig. 17). These results demonstrate the critical role of *Skp2* inactivation in the induction of cellular senescence not only in mouse cells, but also in human cancer cells experiencing failure of p53 and other major tumour-suppressive networks.

Discussion

On the basis of our results, we propose a working model for the role of *Skp2* inactivation-induced cellular senescence in tumour prevention and suppression *in vivo* (Fig. 5f). This model rests on three new and unexpected findings with important therapeutic implications. First, *Skp2* inactivation does not trigger cellular senescence *in vivo* or *in vitro* on its own, but rather elicits a senescence response after oncogenic stress. This response is critically dependent on p27, p21 and Atf4 induction. Our results are supported by recent reports showing that acute inactivation of the von Hippel-Lindau (VHL) tumour suppressor *in vitro* or overexpression of the human T-lymphotropic virus type 1 (HTLV-1) Tax triggers *Skp2* downregulation and cellular senescence^{37,38}. Second, we show that cellular senescence driven by *Skp2* inactivation along with oncogenic insults takes place without the activation of the p19^{Arf}-p53 failsafe pathway. Although senescence is also observed in p53/*Pten*-null cells such as PC3, it will be important to determine the specific genetic states that favour evasion of this failsafe mechanism, also in a cell-type-specific manner. For instance, loss or constitutively low expression of p27, p21 and Atf4 could impair this response. This knowledge will in turn identify new pharmacological nodes of tumour-type-specific intervention. Third, we show that *Skp2* deficiency in conjunction with oncogenic signals elicits a senescence response that profoundly restricts tumorigenesis *in vivo* in numerous mouse models in which tumour suppressor networks are faulty or inactive. Our findings are consistent with a recent report demonstrating that mice transplanted with BCR-ABL-transduced *Skp2^{-/-}* bone marrow cells show a delayed onset of a myeloproliferative syndrome³⁹.

As *Skp2* can in principle be subjected to specific pharmacological inhibition because of its enzymatic activity, our results call for the development and optimization of *Skp2* small molecule inhibitors. *Skp2* pharmacological inhibition could be particularly appealing and

effective in view of the fact that complete *Skp2* inactivation in the mouse is compatible with life, whereas cellular senescence is only triggered by *Skp2* inactivation in conjunction with oncogenic conditions.

METHODS SUMMARY

Pten^{loxP/loxP}, *Arf^{-/-}* and *Skp2^{-/-}* mice were generated as described previously^{2,18,35}. Female *Pten^{loxP/loxP}* mice were crossed with male *PB-Cre4* transgenic mice for the prostate-specific deletion of *Pten*. MEFs from wild-type and *Skp2^{-/-}* mice were prepared as previously described^{40,41} and cultured in DMEM containing 10% FBS. Cellular senescence was determined by assessing SA- β -gal activity, and the *in vivo* cell proliferation assay was performed by Ki67 staining on the paraffin tissue sections. The cell transformation assay was determined by the soft agar assay. p53 shRNA is from S. W. Lowe and the pBabe-p53 dominant-negative construct is a gift from M. Oren. MLN4924 was obtained from Millennium Pharmaceuticals.

Full Methods and any associated references are available in the online version of the paper at www.nature.com/nature.

Received 9 October 2009; accepted 11 January 2010.

1. Sharpless, N. E. & DePinho, R. A. Cancer: crime and punishment. *Nature* **436**, 636–637 (2005).
2. Chen, Z. *et al.* Crucial role of p53-dependent cellular senescence in suppression of *Pten*-deficient tumorigenesis. *Nature* **436**, 725–730 (2005).
3. Xue, W. *et al.* Senescence and tumour clearance is triggered by p53 restoration in murine liver carcinomas. *Nature* **445**, 656–660 (2007).
4. Ventura, A. *et al.* Restoration of p53 function leads to tumour regression *in vivo*. *Nature* **445**, 661–665 (2007).
5. Braig, M. *et al.* Oncogene-induced senescence as an initial barrier in lymphoma development. *Nature* **436**, 660–665 (2005).
6. Michaloglou, C. *et al.* BRAF600-associated senescence-like cell cycle arrest of human naevi. *Nature* **436**, 720–724 (2005).
7. Collado, M. *et al.* Tumour biology: senescence in premalignant tumours. *Nature* **436**, 642 (2005).
8. Cantley, L. C. & Neel, B. G. New insights into tumor suppression: PTEN suppresses tumor formation by restraining the phosphoinositide 3-kinase/AKT pathway. *Proc. Natl Acad. Sci. USA* **96**, 4240–4245 (1999).
9. Di Cristofano, A. & Pandolfi, P. P. The multiple roles of PTEN in tumor suppression. *Cell* **100**, 387–390 (2000).
10. Salmena, L., Carracedo, A. & Pandolfi, P. P. Tenets of PTEN tumor suppression. *Cell* **133**, 403–414 (2008).
11. Bloom, J. & Pagano, M. Deregulated degradation of the cdk inhibitor p27 and malignant transformation. *Semin. Cancer Biol.* **13**, 41–47 (2003).
12. Nakayama, K. I. & Nakayama, K. Regulation of the cell cycle by SCF-type ubiquitin ligases. *Semin. Cell Dev. Biol.* **16**, 323–333 (2005).
13. Gstaiger, M. *et al.* *Skp2* is oncogenic and overexpressed in human cancers. *Proc. Natl Acad. Sci. USA* **98**, 5043–5048 (2001).
14. Latres, E. *et al.* Role of the F-box protein *Skp2* in lymphomagenesis. *Proc. Natl Acad. Sci. USA* **98**, 2515–2520 (2001).
15. Shim, E. H. *et al.* Expression of the F-box protein SKP2 induces hyperplasia, dysplasia, and low-grade carcinoma in the mouse prostate. *Cancer Res.* **63**, 1583–1588 (2003).
16. Lin, H. K. *et al.* Phosphorylation-dependent regulation of cytosolic localization and oncogenic function of *Skp2* by Akt/PKB. *Nature Cell Biol.* **11**, 420–432 (2009).
17. Chiarle, R. *et al.* S-phase kinase-associated protein 2 expression in non-Hodgkin's lymphoma inversely correlates with p27 expression and defines cells in S phase. *Am. J. Pathol.* **160**, 1457–1466 (2002).
18. Nakayama, K. *et al.* Targeted disruption of *Skp2* results in accumulation of cyclin E and p27^{Kip1}, polyploidy and centrosome overduplication. *EMBO J.* **19**, 2069–2081 (2000).
19. Lin, A. W. *et al.* Premature senescence involving p53 and p16 is activated in response to constitutive MEK/MAPK mitogenic signaling. *Genes Dev.* **12**, 3008–3019 (1998).
20. Serrano, M., Lin, A. W., McCurrach, M. E., Beach, D. & Lowe, S. W. Oncogenic *ras* provokes premature cell senescence associated with accumulation of p53 and p16^{INK4a}. *Cell* **88**, 593–602 (1997).
21. Kim, W. Y. & Sharpless, N. E. The regulation of INK4/ARF in cancer and aging. *Cell* **127**, 265–275 (2006).
22. Yaswen, P. & Campisi, J. Oncogene-induced senescence pathways weave an intricate tapestry. *Cell* **128**, 233–234 (2007).
23. Hemann, M. T. *et al.* An epi-allelic series of p53 hypomorphs created by stable RNAi produces distinct tumor phenotypes *in vivo*. *Nature Genet.* **33**, 396–400 (2003).
24. Gottlieb, E., Haffner, R., von Ruden, T., Wagner, E. F. & Oren, M. Down-regulation of wild-type p53 activity interferes with apoptosis of IL-3-dependent hematopoietic cells following IL-3 withdrawal. *EMBO J.* **13**, 1368–1374 (1994).
25. Chen, Z. *et al.* Differential p53-independent outcomes of p19^{Arf} loss in oncogenesis. *Sci. Signal.* **2**, ra44 (2009).
26. Bartkova, J. *et al.* Oncogene-induced senescence is part of the tumorigenesis barrier imposed by DNA damage checkpoints. *Nature* **444**, 633–637 (2006).

27. Di Micco, R. *et al.* Oncogene-induced senescence is a DNA damage response triggered by DNA hyper-replication. *Nature* **444**, 638–642 (2006).
28. Mallette, F. A., Gaumont-Leclerc, M. F. & Ferbeyre, G. The DNA damage signaling pathway is a critical mediator of oncogene-induced senescence. *Genes Dev.* **21**, 43–48 (2007).
29. Yu, Z. K., Gervais, J. L. & Zhang, H. Human CUL-1 associates with the SKP1/SKP2 complex and regulates p21^{CIP1/WAF1} and cyclin D proteins. *Proc. Natl Acad. Sci. USA* **95**, 11324–11329 (1998).
30. Denoyelle, C. *et al.* Anti-oncogenic role of the endoplasmic reticulum differentially activated by mutations in the MAPK pathway. *Nature Cell Biol.* **8**, 1053–1063 (2006).
31. Kim, I., Xu, W. & Reed, J. C. Cell death and endoplasmic reticulum stress: disease relevance and therapeutic opportunities. *Nature Rev. Drug Discov.* **7**, 1013–1030 (2008).
32. Di Cristofano, A. *et al.* Impaired Fas response and autoimmunity in *Pten*^{+/-} mice. *Science* **285**, 2122–2125 (1999).
33. Di Cristofano, A., Pesce, B., Cordon-Cardo, C. & Pandolfi, P. P. *Pten* is essential for embryonic development and tumour suppression. *Nature Genet.* **19**, 348–355 (1998).
34. Kamijo, T., Bodner, S., van de Kamp, E., Randle, D. H. & Sherr, C. J. Tumor spectrum in ARF-deficient mice. *Cancer Res.* **59**, 2217–2222 (1999).
35. Kamijo, T. *et al.* Tumor suppression at the mouse *INK4a* locus mediated by the alternative reading frame product p19^{ARF}. *Cell* **91**, 649–659 (1997).
36. Soucy, T. A. *et al.* An inhibitor of NEDD8-activating enzyme as a new approach to treat cancer. *Nature* **458**, 732–736 (2009).
37. Young, A. P. *et al.* VHL loss actuates a HIF-independent senescence programme mediated by Rb and p400. *Nature Cell Biol.* **10**, 361–369 (2008).
38. Kuo, Y. L. & Giam, C. Z. Activation of the anaphase promoting complex by HTLV-1 tax leads to senescence. *EMBO J.* **25**, 1741–1752 (2006).
39. Agarwal, A. *et al.* Absence of SKP2 expression attenuates BCR-ABL-induced myeloproliferative disease. *Blood* **112**, 1960–1970 (2008).
40. Lin, H. K., Bergmann, S. & Pandolfi, P. P. Cytoplasmic PML function in TGF- β signalling. *Nature* **431**, 205–211 (2004).
41. Yang, W. L. *et al.* The E3 ligase TRAF6 regulates Akt ubiquitination and activation. *Science* **325**, 1134–1138 (2009).

Supplementary Information is linked to the online version of the paper at www.nature.com/nature.

Acknowledgements We are grateful to C. J. Sherr, S. W. Lowe and M. Oren for mice and reagents. We would also like to thank B. Carver, L. DiSantis, J. Clossey and S. Megan for editing and critical reading of the manuscript, J. A. Koutcher, C. Le, C. Matei and M. Lupa for MRI analysis, as well all the members of the Pandolfi laboratory for comments and discussion. We extend our thanks to M. Rolfe, P. G. Smith, and Millennium Pharmaceuticals for discussion and for providing the MLN4924 compound. This work was supported by NIH grants to P.P.P. and M.D. Anderson Trust Scholar Award and DOD Prostate Cancer New Investigator Award to H.K.L.

Author Contributions H.K.L. and P.P.P. designed the experiments and wrote the manuscript; H.-K.L., Z.C., G.W., S.-W.L., C.N., C.-H.C., W.-L.Y., J.W. and A.E. performed the experiments; C.C.-C. and J.T.-F. performed the histopathological analysis of the mice; K.I.N. provided the *Skp2*^{-/-} mice.

Author Information Reprints and permissions information is available at www.nature.com/reprints. The authors declare no competing financial interests. Correspondence and requests for materials should be addressed to P.P.P. (ppandolf@bidmc.harvard.edu).

METHODS

shRNA-mediated silencing. For the retrovirus-infection system, *p27* shRNA (5'-GTGGAATTCGACTTTCAG-3'), *Atf4* shRNA (5'-GAGCATTCCCTTAGTTAG-3'), and GFP shRNA (5'-GCAAGCTGACCCTGAAGTTC-3') were sub-cloned into the pSUPER-puro vector (Oligoengine) according to standard procedures and transfected into Phoenix packaging cells. For lentiviral shRNA infection, 293T cells were co-transfected with *p27*, *Atf4*, *p21*, *Skp2* or GFP control shRNA along with packing plasmids (Δ VPR8.9) and envelope plasmid (VSV-G) using Lipofectamine 2000 reagents according to the manufacturer's instructions. *Skp2*-lentiviral shRNA-1 (5'-GATAGTGTATGCTAAAGAAT-3'), *p27*-lentiviral shRNA-1 (5'-CGCAAGTGGAAATTCGACTTT-3'), *p27*-lentiviral shRNA-2 (5'-CCCGGTCAATCATGAAGAACT-3'), *Atf4*-lentiviral shRNA-1 (5'-GCGAGTGTAAGGAGCTAGAAA-3'), *Atf4*-lentiviral shRNA-2 (5'-CGGACAAAGATACCTTCGAGT-3'), *p21*-lentiviral shRNA-1 (5'-CTGGTGTCTGAGCGGCCTGAA-3'), *p21*-lentiviral shRNA-2 (5'-GACAGATTTCTATCACTCCAA-3'), and GFP shRNA (5'-GCAAGCTGACCCTGAAGTTC-3') were transfected with packing plasmids into 293T cells for 2 days, and virus particles containing *p27*, *p21*, *Atf4*, *Skp2* or GFP shRNA were used to infect mammalian cells. All the infected cells were cultured in a medium containing the appropriate antibiotics.

Western blot analysis and immunohistochemistry. Cell lysates were prepared with RIPA buffer (PBS, 1% Nonidet P40, 0.5% sodium deoxycholate, 0.1% SDS and protease inhibitor cocktail (Roche)). The following antibodies were used for western blot analysis: anti-p19^{Arf} (NeoMarkers), anti-p53 (Novocastra), anti-p21 (Santa Cruz), anti- β -actin (Sigma), anti-Hsp90 (BD transduction laboratories), anti-p27 (BD transduction laboratories), anti- α -tubulin (Sigma), anti-phospho-p53 (Ser15) (Cell Signaling), anti-phospho-H2ax (Ser139) (Cell Signaling), anti-phospho-eIF2 α (Ser51) (Cell Signaling), anti-eIF2 α (Cell Signaling), anti-phospho-Perk (Thr980) (Cell Signaling), anti-cyclin D1 (Santa Cruz), anti-E2F1 (Santa Cruz), anti-Cdt1 (Proteintech Group), anti-Ras (Oncogene), anti-E1A (NeoMarkers), and anti-Atf4 (Santa Cruz). For immunohistochemistry, tissues were fixed in 10% formalin and embedded in paraffin in accordance with standard procedures. Sections were stained with anti-p27 (BD transduction

laboratories), anti-Ki67 (Novocastra), anti-Pten (Neomarkers) and anti-p53 (Novocastra) antibodies.

Cell proliferation, transformation and senescence. Primary MEFs were isolated from individual embryos of various genotype at passage 2, infected with retroviruses or lentiviruses expressing GFP shRNA, *p27* shRNA or *Atf4* shRNA for 2 days, selected with 2 μ g ml⁻¹ puromycin for 4 days, and plated for the cell proliferation and senescence assay. For cell proliferation assay, 2 \times 10⁴ MEFs were seeded in 12 wells in triplicate, collected, and stained with trypan blue at different days. Numbers of viable cells were directly counted under the microscope. To determine cellular senescence, MEFs were plated at 10⁴ cells per well of a 6-well plate in triplicate, and after 4 days SA- β -gal activity was measured using the senescence detection kit (Calbiochem) and quantified (around 100–200 cells per well). For *in vivo* cellular senescence, frozen sections 6- μ m thick were stained for β -gal as described earlier. For *in vivo* cell proliferation, the paraffin section was used for Ki67 staining, and the percentages of Ki67-positive cells (around 500 cells) from each sample were counted. For transformation assay, wild-type and *Skp2*^{-/-} MEFs (3 \times 10⁴) infected with Ras(G12V) and E1A were suspended in a medium containing 0.3% agar onto solidified 0.6% agar per well of a 6-well plate, and the number of colonies was counted after 21 days.

Apoptosis assay. Primary MEFs of various genotypes of mouse embryos were cultured in 10% FBS for 2 days; cells were collected and labelled with Annexin-V-FITC, followed by a flow cytometry analysis.

MRI. Individual mice were subjected to MRI assessment for the detection of prostate tumours as described⁴².

***In vivo* drug treatment in the preclinical tumour model.** Nude mice bearing PC3 xenograft tumours (around 300 mm³) were treated with vehicle or 90 mg kg⁻¹ MLN492. Tumour weight was measured at the time of collection after 15 days of treatment with a scheduling regimen of 3 days of treatment followed by 3 days without treatment for a total of three courses.

42. Chen, Z. *et al.* Crucial role of p53-dependent cellular senescence in suppression of Pten-deficient tumorigenesis. *Nature* 436, 725–730 (2005).

CORRIGENDUM

doi:10.1038/nature09280

***Skp2* targeting suppresses tumorigenesis by
Arf-p53-independent cellular senescence**

Hui-Kuan Lin, Zhenbang Chen, Guocan Wang, Caterina Nardella,
Szu-Wei Lee, Chia-Hsin Chan, Wei-Lei Yang, Jing Wang,
Ainara Egia, Keiichi I. Nakayama, Carlos Cordon-Cardo,
Julie Teruya-Feldstein & Pier Paolo Pandolfi

Nature 464, 374–379 (2010)

In this Article, author Chia-Hsin Chan was incorrectly listed as Chan-Hsin Chan.